# OECD INTERNATIONAL STANDARD PROBLEM ISP-50 ON THE ATLAS DVI LINE BREAK TEST

**Ki Yong Choi[1], Won-Pil Baek, Hyun-Sik Park, Seok Cho, Kyoung-Ho Kang, and Yeon-Sik Kim**

[1]Thermal Hydraulics Safety Research Division,
Korea Atomic Energy Research Institute
1045 Daedeokdaero, Yuseong, Daejeon 305-353, Korea
Phone: +82 (42) 868-8928, Fax: +82 (42) 861-6438, E-Mail:kychoi@kaeri.re.kr

## Abstract

An international standard problem (ISP) exercise, ISP-50 was progressed with the Advanced Thermal-Hydraulic Test Loop for Accident Simulation (ATLAS) integral effect test results on 50% break of the cross section of a Direct Vessel Injection (DVI) nozzle of the APR1400. This exercise consisted of two serial phases: blind and open calculation. In the open calculation, a total of 16 calculations was collected from 11 organizations and seven leading safety analysis codes were used, including APROS, ATHLET, KORSAR, MARS-KS, RELAP5/MOD3, CATHARE, and TRACE. Local 3-D phenomena such as a down-comer mixing, a radial peak cladding temperature (PCT) distribution, and an asymmetric inventory distribution were highlighted in this exercise. Overall progress of the ISP-50 is outlined in this paper.

## 1. Introduction

Korea Atomic Energy Research Institute (KAERI) has been operating an integral effect test facility, the ATLAS for accident simulations for the OPR1000 and the APR1400 which are in operation or under construction in Korea, respectively. [1]. The ATLAS program started in 1997 under a nuclear R&D mid- and long-term project funded by the Korean government. Since a complete installation of the ATLAS in 2005, intensive tests on the LBLOCA reflood phase were performed in 2007 [2].

The DVI-adopted plants treat a DVI line break as another spectrum among the small break loss of coolant accidents (SBLOCAs) in their safety analysis because a DVI nozzle directly attached to a reactor pressure vessel (RPV) down-comer is vulnerable to a postulated break from a safety viewpoint. The thermal hydraulic phenomena in the RPV down-comer expecting to occur in the DVI line break scenario are believed to be different from the cold leg injection (CLI) plants. In the event of a DVI line break, the vapor generated in the core is introduced to the RPV down-comer through the hot legs, the steam generators and the cold legs. Then the vapor should pass through the upper part of the RPV down-comer to be discharged through the broken DVI nozzle. Therefore, the behavior of the two-phase flow in the upper annulus down-comer is expected to be complicated and relevant models need to be implemented into safety analysis codes in order to predict these thermal hydraulic phenomena correctly. So far there is not enough integral effect test data for the DVI line breaks which can demonstrate the progression of the DVI line break accident realistically. The test data for the DVI line breaks can be used for an assessment and improvement of safety analysis codes. Hence, sensitivity tests for different DVI line break sizes were successfully performed in 2008 [3,4].

Among the DVI line break scenarios, 50% of the cross section of a DVI nozzle is of technical interest because this break size is on the edge of the criterion provided by the EPRI requirement where a core uncovery should be prevented by a best-estimate methodology. In particular, the thermal-hydraulic phenomena occurring in the upper annulus down-comer region between the DVI nozzle and the cold leg nozzles are expected to be 3-dimensional due to the countercurrent flow of the upward break flow and the downward safety injection flow. Therefore, the relevant models need to be incorporated into the safety analysis codes in order to predict these thermal hydraulic phenomena correctly.

In the present ISP-50 exercise, the predictions of a 50% DVI line break accident of the APR1400 by different best-estimate computer codes were compared with each other and above all with the carefully specified experimental data. This exercise has contributed to assessing the code's modeling capabilities and to identifying any deficiencies of the best-estimate system codes of the participants against the obtained integral effect test data on the DVI line break accident.

The present ISP exercise was performed in two phases. In the phase 1, ISP exercise was performed as a "blind" problem. The experimental results were locked except for actual test conditions and procedure until the calculation results were made available for a comparison. In the following phase 2, the ISP exercise was performed as an "open" problem with the experimental results released to the participants. And a post-test calculation was performed based on the released experimental data.

## 2. Outline and history of the ISP-50

The ATLAS was utilized to provide the unique integral effect test data for the 2(hot legs) x 4(cold legs) reactor coolant system with a DVI of emergency coolant; this integral effect test significantly expanded the currently available database for code validation. The ISP exercise using the ATLAS database is expected to significantly contribute to the enhancement of understanding on the behavior of nuclear reactor systems with the DVI and to the assessment of existing and new thermal-hydraulic analysis codes such as TRACE, CATHARE, RELAP, TRAC, ATHLET, CATHENA, MARS, etc.

The ISP exercise using the ATLAS facility was proposed and discussed at the 10th Plenary Meeting of the NEA Committee on the Safety of Nuclear Installations (CSNI) Working Group on Analysis and Management of Accidents (WGAMA) in September 2007. The discussion at the GAMA plenary meeting with possible participants revealed that a DVI line break scenario would be attractive for the ISP exercise. At the 11th WGAMA meeting in October 2008, KAERI submitted a specified ISP proposal and a relavent CAPS (CSNI Activity Proposal Sheet) as well based on a DVI line break scenario for Program Review Group (PRG) approval, after final endorsement by WGAMA members. Subsequently, the ISP exercise with the ATLAS facility focusing on a DVI line break scenario was finally approved by the CSNI meeting in December 2008 and was numbered by ISP-50.

The first workshop (kick-off meeting), where 11 organizations attended, was held at KAERI in April, 21-22, 2009 to finalize the ISP-50 specifications. As agreed at the first workshop, ISP-50 working page (www.oecd-nea.org/download/isp-50) was constructed and opened under NEA web site in May, 2009. The specification was finalized by incorporating answers to the questions and comments on the proposed specifications and it was distributed in June, 2009. An updated facility description report and a data submission format were also sent to all the participants. The agreed test was successfully performed by the operating agency, KAERI in July, 2009. In fact, this was a repeatability test for the test which was done a year ago. Excellent agreement between two tests was confirmed. Information document on actual test conditions and procedure was distributed in August, 2009. The submission due date for the “blind” calculation was extended to January, 16, 2010 by two weeks to take into account the final schedule.

In the “blind” calculation, a total of 17 calculation results was submitted from 13 organizations. A few participants showed their intentions to join the following “open” calculation phase due to lack of available resources. Seven leading safety analysis codes were used in the “blind” phase, including RELAP5/MOD3, TRACE, MARS-KS, KORSAR, TECH-M-97, APROS, and ATHLET. The second workshop was held at OECD headquarter in May 25-26, 2010 to present and to discuss the blind calculation results and future steps. Experimental results and overview of the comparison of the calculation results were presented by the operating agency. Quantitative comparison of the submitted calculations by Fast Fourier Transform Based Method (FFTBM) was also presented and discussed. Detailed presentations of eleven blind calculation results continued. The participants also discussed the parameters for which a comparison of calculated and experimental results would be interesting as well as the physical phenomena in down-comer and loop seal clearing. In particular 3D phenomena (e.g., temperature distribution, flow in the down-comer) may be of prime interest. Temperature and condensation rates at injection points, differential pressures, and void fraction distribution (e.g., in the down-comer and in the core) were suggested. JAEA and NRC accepted to help KAERI to point out the 3D behaviour in the down-comer and in the core. Some participants expressed the need for additional information in order to improve their understanding and interpretation of the test and hence in order to improve their calculation results in the post-test phase. It was agreed that the participants would send their requests to KAERI in written form. KAERI compiled the requests and analyzed the requests and answered by issuing detailed test report for 50% DVI line break simulation.

The post-test calculation, the “open” phase program started after the second workshop. The operating agency prepared an experimental data in a much extended format and uploaded it on the ISP-50 website. A total of 269 parameters for major thermal hydraulic variables were open to the participants. Detailed cladding temperatures for 264 different locations inside the core were also distributed to the participants. In addition, the operating agency delivered specifications for output submission, where 144 of 269 parameters were requested. PSI (Switzerland) and AEKI/KFKI (Hungary) took part in this “open” calculation. Sixteen calculation results were collected from October, 2010 to March, 2011. As the CATHARE code was used by AEKI/KFKI and the calculation by the TECH-M-97 code (GP4) was not submitted in the “open” phase, the number of code used in the ISP-50 was seven: RELAP5/MOD3, TRACE, MARS-KS, KORSAR, APROS, CATHARE, and ATHLET. A final integration report was prepared with help of participants by the operating agency to incorporate the results in the “blind” phase.

A best-estimate safety analysis methodology for the DVI line break accidents needs to be developed to identify the uncertainties involved in the safety analysis results. Such best-estimate safety analysis methodology will contribute to defining a more precise specification of safety margins and thus lead to a greater operational flexibility. However, such an effort has never been reported yet due to a lack of an integral effect database on the DVI line break accidents.

The current ATLAS ISP-50 aims at; 1) better understanding of thermal-hydraulic phenomena in the upper annulus down-comer region during the DVI injection period, 2) generation of integral effect database for code development and validation, 3) investigation of the possible limitation of the existing best-estimate safety analysis codes.

## 3. Organization

The ATLAS ISP-50 was led by KAERI in collaboration with OECD/NEA. KAERI was responsible for general coordination of the ISP-50, data provision, information on the ATLAS and the ISP-50, code calculation, receipt of submissions, results comparison, progress meetings, final workshop, and comparison report. Organizations of the ATLAS ISP-50 program are as listed in Table 1. A few organizations joined the "open" calculation phase followed by the "blind" calculation phase. Each signed organization had an obligation to perform an open calculation within the calculation period by using the test results which were provided by the operating agency, KAERI. All the participants were also requested to write their analysis results in an assigned section of a final comparison report.

Table 1 List of participants

| Country | Organization | Participants | Code |
|---|---|---|---|
| China | CIAE[1)] | Chen Yuzhou; chenyz@ciae.ac.cn | RELAP5/MOD3.3 |
| Czech Republic | NRI | Radim Meca; mec@ujv.cz | ATHLET |
| Finland | VTT | Pasi Inkinen; Pasi.Inkinen@vtt.fi | APROS 5.09 |
| | FORTUM | Ahonen Aino; Aino.Ahonen@fortum.com | APROS v.5.08 |
| Germany | GRS | Henrique Austregesilo; Henrique.Austregesilo@grs.de | ATHLET Mod 2.2 Cycle A |
| Hungary | AEKI/KFKI | Antal Takacs; takacs@aeki.kfki.hu | CATHARE 2V1.5Bmod3.1 |
| Italy | U. of Pisa | Marco Cherubini; m.cherubini@ing.unipi.it | RELAP5/MOD3.3 |
| Russia | EDO Gidropress | Vladimir Schekoldin Schekoldin_vv@grpress.podolsk.ru | KORSAR TRAP |
| Sweden | KTH | Erdenechimeg Suvdantsetseg and Tomasz Kozlowski; tomasz@safety.sci.kth.se | TRACE 5.0 patch 1 |
| Switzerland | PSI | Annalisa Manera; Annalisa.manera@psi.ch Medhat Sharabi; | RELAP5/MOD3.3 |

| | | | |
|---|---|---|---|
| | | Medhat.sharabi@psi.ch | |
| USA | NRC | Harrington Ronald;<br>Ronald.Harrington@nrc.gov<br>Scott Krepel;<br>Scott.krepel@nrc.gov | TRACE 5.200<br>TRACE 5.0 patch 2 |
| Korea | KAERI | K. D. Kim; kdkim@kaeri.re.kr | MARS-KS |
| | KNF | T. S. Choi; tschoi@knfc.co.kr | RELAP5/MOD3.3 |
| | KEPRI | S. J. Ha; hsj@kepri.re.kr<br>S.Y. Kim; seyunkim@kepri.re.kr | MARS-KS |
| | KOPEC | C. W. Kim; cwkim@kopec.co.kr<br>H. R. Choi; hrchoi@kopec.co.kr<br>Y.M. Kim; kimym@kopec.co.kr | RELAP5-ME<br>RELAP5/MOD3.3 |

## 4. Comparison results

### 4.1 Pre-test calculation

Seventeen calculation results were finally submitted for the "blind" calculation of the ISP-50. Seven different safety analysis codes were used: MARS-KS, TRACE, RELAP5/MOD3.3 series, KORSAR, TECH-M-97, APROS and ATHLET. The prediction accuracy of the initial conditions was acceptable by taking into account the "blind" exercise. All the calculations qualitatively succeeded in simulating the typical transient behaviors during the DVI line break accident, including the primary pressure depressurization, primary pressure plateau, the Main Steam Safety Valve (MSSV) opening, loop seal clearing, RPV core water level depression, and break flow. However, a few participants seemed not to have full understanding of the actual test conditions. A certain boundary conditions, for instance, the core power with respect to time or ECC flow rate, were not properly implemented in the code calculations.

On the whole, the prediction accuracy of each thermal-hydraulic phenomenon was not satisfactory. In particular, prediction discrepancy of the RPV core and down-comer level was significant in most calculations. The safety injection tank (SIT) flow rate was also not properly predicted by most calculations. As expected, the break flow rate was not predicted well since two-phase break flow itself has many uncertainties in measurement and model as well.

Prediction accuracy quantification was performed by applying the FFTBM to the submitted calculations. Detailed methodology was determined by communicating with the Univ. of Pisa, by which the FFTBM was developed. 22 parameters were carefully selected to capture all major thermal-hydraulic phenomena and to avoid duplication of variables. Three time intervals were selected by taking into account the transient phases defined in the Phenomena Identification and Ranking Tabulation (PIRT) process. The first time interval corresponded to the pre-trip phase. The calculation results before the decay of the core power were considered. In the second time interval, the transient behavior before the injection of the ECC water from the SITs was considered. Finally, the transient up to 2000 s was taken to be the third time interval. On the whole, the prediction accuracy became worse as the time interval became longer.

### 4.2 Post-test calculation

### 4.2.1 Initial and boundary conditions

The initial and boundary conditions used by all the calculations are listed in Table 4. Major thermal hydraulic parameters were selected and compared with the data. It can be found that most initial and boundary conditions agreed with the experimental values.

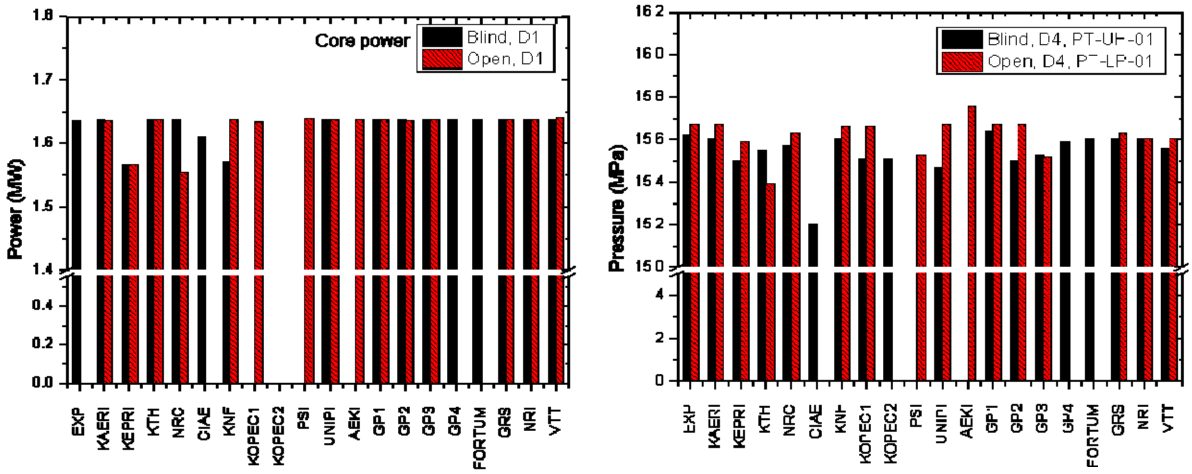


Figure 1 Comparison of initial core power and primary pressure

### 4.2.2 Nodalization scheme and sequence of events

Most calculations were performed by one dimensional modeling, but multi-dimensional modeling on the down-comer and the reactor pressure vessel was done by some participants. Most participants applied two-dimensional modeling to the down-comer region. When multiple channels were used to take into account the effects of cross flow between two adjacent channels, this modeling can be treated as two-dimensional. The number of azimuthal sections showed a variation from 4 to 8 depending on calculations. As for the reactor pressure vessel, KTH and USNRC applied a 3-D VESSEL component in order to predict the 3-D behavior of the peak cladding temperature.

Number of nodalization showed a wide range of variation. KTH used the greatest number of volumes, 863 volumes, to model the ATLAS facility with the TRACE code. USNRC who used the same TRACE code used 94 volumes except for the 3-D VESSEL component. UNIPI used 823 volumes with RELAP5/MOD3.3 code. VTT used 592 volumes with the APROS code. On average, the number of volumes used by the other participants ranges around 100 and 300. Number of heat structures showed a great difference. KTH used the minimum number of heat structures but VTT used the maximum of 1866.

### 4.2.3 Steady state comparison

Comparisons of steady state results for the major thermal-hydraulic parameters were made. Figure 1 shows a comparison of the initial core power and pressure. Depending on whether the primary heat loss was taken into account in the code model, difference in the calculated core power was observed. For instance, KEPRI excluded the additional power for compensating the primary heat loss in his model, resulting in around 1.56 MW. It is interesting that NRC and KNF changed their modeling strategy in the open calculation. NRC included the additional core power for the primary heat loss in the blind calculation but excluded it in the open calculation. KNF took the opposite strategy between two calculations. How the heat loss effects can be treated in the code model is open to dispute. However, most participants were in favor of inclusion of the additional core power for heat loss compensation in their model. In the open calculation, the PT-LP-01 was used as a representative primary pressure instead of PT-UH-01 in the previous calculation. Therefore, pressure from PT-LP-01 has higher value than that for PT-UH-01. However, a few organizations produced lower primary pressures than those in the blind case. Calculated primary pressures show a variation from 15.39 MPa (KTH) to 15.76 MPa (AEKI).

The submitted core inlet temperatures are close to the measured data and the minimum is 561.9 K by UNIPI and the maximum is 566.7 K by AEKI. NRI and VTT presented better values than the blind case. As for the core exit temperature, most calculations are in very good agreement with the data. The improvement by KOPEC1 is remarkable.

Regarding the down-comer-to-upper head and down-comer-to-hot leg bypass flow rate, note that many organizations – KEPRI, KNF, KOPEC1, PSI, UNIPI, GRS, VTT – predicted negative down-comer-to-upper head flow rate. NRI's calculation showed a little higher down-comer-to-upper head flow rate than that in the case of open calculation. On the other hand, the predicted down-comer-to-hot leg bypass flow rate was always positive which is consistent with experimental observation. Most calculations agree well with the data in the open phase. But, GP1 predicted enhanced bypass flow rate in the open phase compared with the blind phase.

As for the secondary pressure, there was no significant difference between the blind and the open calculations. Overall, KAERI's prediction was a little lower than the data. Better agreement can be observed in the predictions by KNF and GP2. Most predictions of the secondary economizer feedwater flow are in good agreement with the data. In particular, the NRI's prediction was much improved compared with the blind case. Incorrect predictions of the down-comer feedwater flow rate in the blind phase were improved except for the KEPRI's calculation. The initial pressure and temperature of the SIT-1 and the coolant temperature of the SIP-1 were well reproduced in most calculations because the measured values were provided as initial and boundary conditions. Finally, as for the containment pressure comparison, though the prediction by PSI shows a little higher value than the data, most predictions are well consistent with the data.

### 4.2.4 Transient comparison

Typical prediction results of primary and secondary pressures are shown in Figure 2. Most participants successfully reproduced the primary pressure behaviours. However, the secondary pressure was over-predicted by most calculations. Incorrect prediction of the secondary pressure caused different timing of the opening of the MSSVs. The prediction of break flow and the PCT is shown in Figure 3. There was a wide variation among participants in prediction of the discharge of two-phase mixture observed in the earlier phase prior to the loop seal clearing. As for the PCT, several calculations resulted in much higher delayed PCT than the test data and the non-uniform radial distribution of the PCT was not correctly obtained in any code. On average, the collapsed water levels of the core and the downcomer regions were lower than the data as shown in Figure 4.

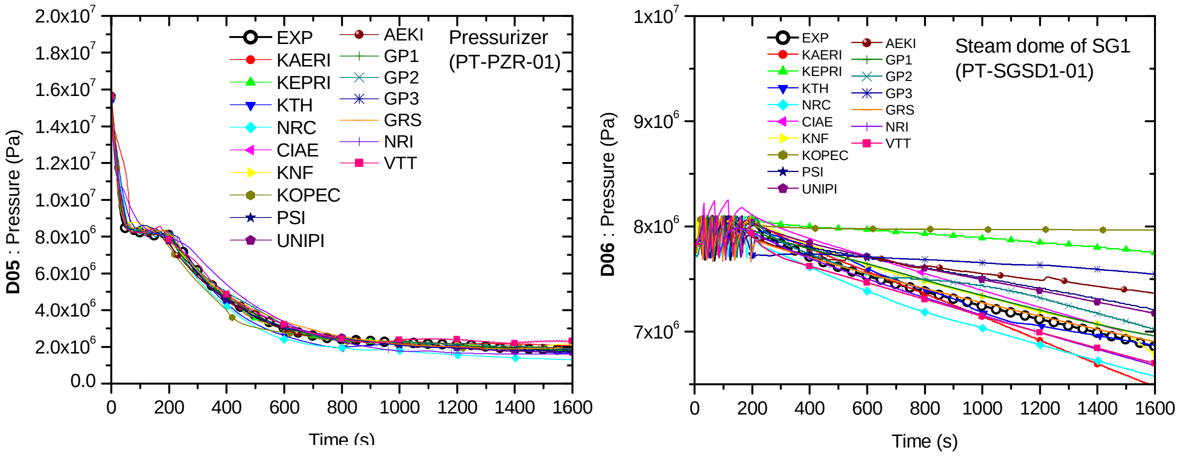


Figure 2 Comparison of primary and secondary pressures

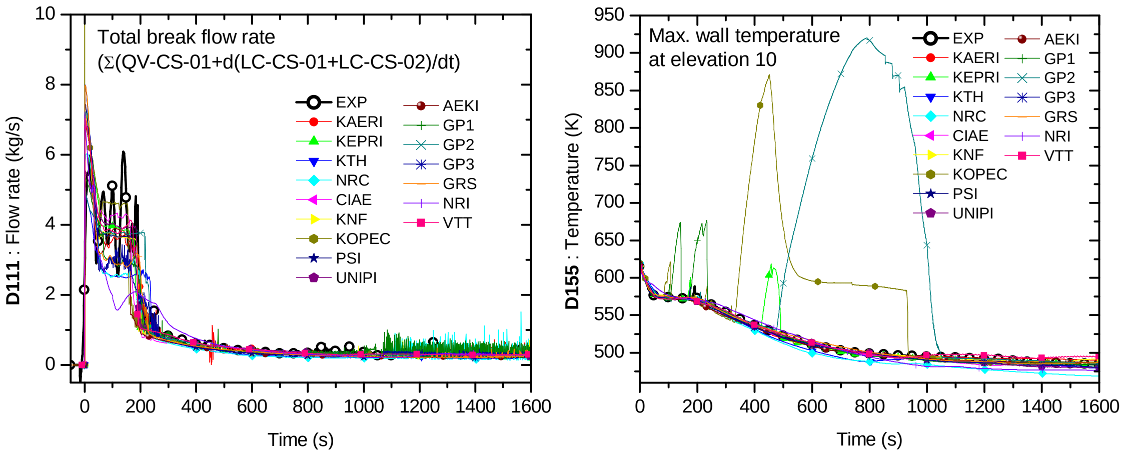


Figure 3 Comparison of break flow and PCT

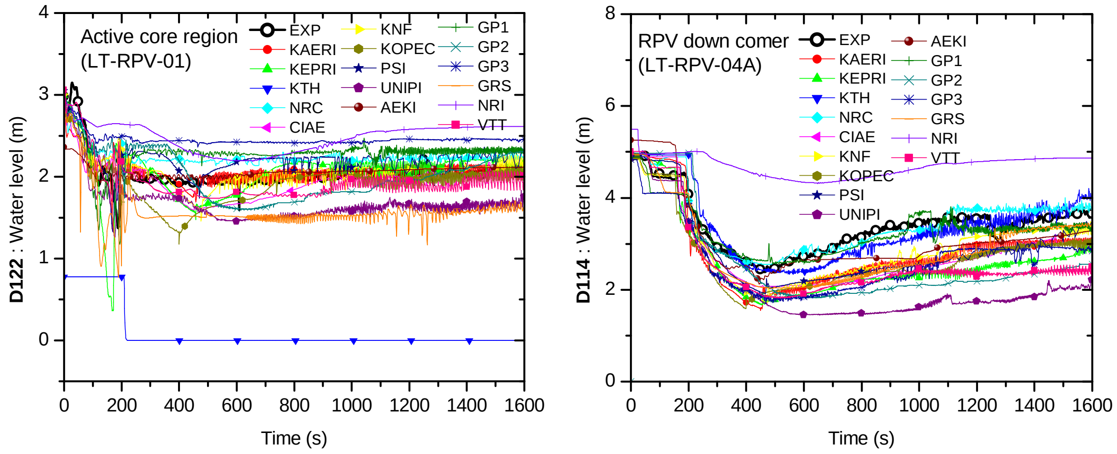


Figure 4 Comparison of the collapsed core and downcomer water levels

## 5. Quantitative comparison by FFTBM

The FFTBM developed by the University of Pisa (DCMN) has been widely applied to the International Standard Problems in order to quantify the accuracy of the code prediction for a given problem [5]. The full FFTBM method requires 20-25 parameters selected representing relevant thermal-hydraulic aspects. By communication with Prof. D'Auria's group, 22 parameters were selected to characterize all the relevant phenomena that were measured during the experiment. Similar parameters which would affect the analysis results and the parameters which have much measurement uncertainties were avoided in this selection process. As shown in Table 2, three time intervals were used based on the PIRT results on the DVI line break.

Table 2 Selected time of interval for FFTBM

| Time of interval | Phase relevant to PIRT | Phenomena observed | # of data | Max. frequency (Hz) |
|---|---|---|---|---|
| 0~24 s | Pre-trip | Before the core decay | 512 | 10.66 |
| 0~230 s | Post-trip | Before the SIT injection | 1024 | 2.23 |
| 0~1000 s | Refill and long term cooling | All the interesting phenomena are included in this time frame | 2048 | 1.02 |

The first time interval corresponded to the pre-trip phase up to 24 s. The calculation results before the decay of the core power were considered. In the second time interval up to 300 s, the transient behavior before the injection of the ECC water from the SITs was considered. Finally, the transient up to 2000 s was taken to be the third time interval. The same weighting factors and cut-off frequency were used in the ISP-50. For convenience, improvement of the prediction accuracy was defined as $I = (AA_{tot,open} - AA_{tot,blind}) / AA_{tot,blind}$. Negative value of I indicates an improvement in prediction accuracy based on FFTBM and positive I means a worse in prediction accuracy. This 'I' value was included in the comparison table of Table 3. It can be seen from these figures that better prediction accuracy than the blind calculations was obtained in the open calculations.

Table 3 Improvement of $AA_{tot}$ between blind and open calculation

| Grp. | Partic'nt | Time of interval | | | | | | | | |
|---|---|---|---|---|---|---|---|---|---|---|
| | | 0 ~ 24 s | | | 0~ 300 s | | | 0 ~ 2000 s | | |
| | | N=512 | | | N=1024 | | | N=4096 | | |
| | | blind | open | I(%) | blind | open | I(%) | blind | open | I(%) |
| A | KAERI | 0.1 | 0.110 | **10.0** | 0.25 | 0.210 | **-16.0** | 0.333 | 0.322 | **-3.3** |
| | KEPRI | 0.134 | 0.123 | **-8.2** | 0.271 | 0.213 | **-21.4** | 0.34 | 0.359 | **5.6** |
| | KTH | 0.147 | 0.137 | **-6.8** | 0.298 | 0.241 | **-19.1** | 0.417 | 0.353 | **-15.3** |
| | USNRC | 0.121 | 0.076 | **-37.2** | 0.218 | 0.162 | **-25.7** | 0.32 | 0.348 | **8.8** |
| B | CIAE | 0.093 | 0.092 | **-1.1** | 0.112 | 0.135 | **20.5** | 0.196 | 0.201 | **2.6** |
| | KNF | 0.122 | 0.097 | **-20.5** | 0.158 | 0.159 | **0.6** | 0.331 | 0.302 | **-8.8** |
| | KOPEC1 | 0.403 | 0.096 | **-76.2** | 0.385 | 0.229 | **-40.5** | 0.672 | 0.372 | **-44.6** |
| | KOPEC2 | 0.402 | - | **-** | 0.398 | - | **-** | 0.634 | - | **-** |
| | PSI | - | 0.091 | **-** | - | 0.160 | **-** | - | 0.262 | **-** |
| | UNIPI | 0.118 | 0.067 | **-43.2** | 0.22 | 0.187 | **-15.0** | 0.267 | 0.278 | **4.1** |
| C | AEKI | - | 0.099 | **-** | - | 0.243 | | - | 0.265 | **-** |
| | GP1 | 0.08 | 0.078 | **-2.5** | 0.383 | 0.192 | **-49.9** | 0.444 | 0.324 | **-27.0** |
| | GP2 | - | 0.115 | **-** | - | 0.251 | **-** | - | 0.379 | **-** |
| | GP3 | - | 0.107 | **-** | - | 0.171 | **-** | - | 0.352 | **-** |
| | GP4 | 0.155 | - | **-** | 0.317 | - | **-** | 0.546 | - | **-** |
| D | FORTUM | 0.086 | - | **-** | 0.249 | - | **-** | 0.397 | - | **-** |
| | GRS | 0.102 | 0.109 | **6.9-** | 0.222 | 0.206 | **-7.2** | 0.411 | 0.310 | **-24.6** |
| | NRI | 0.124 | 0.127 | **2.4** | 0.213 | 0.216 | **1.4** | 0.405 | 0.316 | **-22.0** |
| | VTT | 0.113 | 0.090 | **-20.4** | 0.251 | 0.211 | **-15.9** | 0.384 | 0.298 | **-22.4** |

In the first time frame (0 s to 24 seconds), the calculated total weighted average amplitude ($AA_{tot}$) showed more or less the similar values as the blind cases. But, the KOPEC1's calculation showed a significant improvement among the other calculations. In the open calculation phase, all the calculations showed excellent prediction accuracy where $AA_{tot}$ values were less than 0.1.

In the second time frame, great improvement can also be seen from the figure. Most calculations have $AA_{tot}$ values near 0.2. In the third time frame, it is noteworthy that KOPEC1 showed an improvement of 44.6%. They are GP1, GRS, NRI, and VTT that showed improvement around 25%. Meanwhile, KEPRI, NRC, CIAE, and UNIPI showed a little worse calculation results compared with the blind calculations.

Detailed distribution of AA for each calculation was also investigated. The parameters which were not predicted well are hot leg flow rate, SIT flow rate and the collapsed water level in the intermediate legs. This finding was also mentioned in the previous blind calculation. Though a little improvement was observed in the open calculation phase, these parameters are still dominant factors to degrade the total prediction accuracy. Relatively, the critical flow was well predicted. It seems that most participants used their own expertise to obtain the same break flow rate as the data. It was also found that prediction of the behavior of the collapsed water levels was much improved.

## 6. Conclusion

In the ISP-50 program, current status of the performance of leading one-dimensional codes was evaluated against the unique 50% DVI line break data obtained from the ATLAS. Most code predictions showed much improved accuracy in the open phase. As the same code was used by several participants, user effects were observed. In particular, three-dimensional behavior such as down-comer temperature distribution showed great variations in the submitted calculations even though in the same code. The one-dimensional code did not predicted mixing of the cold ECC water with the hot inventory inside the annulus down-comer region. Rather than mixing, an azimuthal stratification was predicted. Asymmetric loop seal clearing behavior brought about difficulty in code prediction. Some calculation succeeded in predicting 1st loop seal clearing, but any calculation did not reproduce the 2nd loop seal clearing.

The FFTBM was applied to calculation results. Most open calculations resulted in very good prediction results. In the third time frame from break to 2000 seconds, the calculated $AA_{tot}$ was around 0.3. Compared with the “blind” case, the improvement of $AA_{tot}$ was more than 20%. A maximum of 45% improvement was observed in a certain calculation. Although a few calculations resulted in worse output than the “blind” case, it was not a big deal. Such degradation in the prediction accuracy was so small that it was very hard to reach any technical conclusion. Having the calculation results, it can be postulated that most participants used their experience and expertise to correct their pre-test calculations. This correction was made in tuning and nodalization to reach better agreement between the data and the calculation.

## 7. References

[1] W. P. Baek, C. H. Song, B. J. Yun, T. S. Kwon, S. K. Moon, and S. J. Lee, “KAERI Integral Effect Test Program and the ATLAS Design,” Nuclear Technology, Vol. 152, 2005, pp.183-195.

[2] H. S. Park, K. Y. Choi, S. Cho, K. H. Kang, Y. S. Kim, and W. P. Baek, “An Integral Effect Test on the LBLOCA Reflood Phenomena for the APR1400 using ATLAS under a Best-Estimate Condition,” Journal of Nuclear Science and Technology, Vol. 46, 2009, pp.1059-1069.

[3] K. Y. Choi, H. S. Park, S. Cho, K. H. Kang, N. H. Choi, D. H. Kim, C. K. Park, Y. S. Kim, and W. P. Baek, "Experimental Simulation of a Direct Vessel Injection Line Break of the APR1400 with the ATLAS," Nuclear Engineering and Technology, Vol. 41, 2009, pp.655-676.

[4] K. Y. Choi, H. S. Park, S. Cho, K. H. Kang, N. H. Choi, W. P. Baek, and Y. S. Kim, "Effects of Break Size on DVI Line Break Accidents of the ATLAS," accepted for Nuclear Technology, 2011.

[5] A. Prosek, F. D'Auria, B. Mavko, "Review of Quantitative Accuracy Assessments with Fast Fourier Transform Based Method (FFTBM)," Nuclear Engineering and Design, Vol. 217, 2002, pp.179-206.

Table 4 Comparison of initial conditions in open calculations

| | Experiment | data column | Group A | | | | Group B | | | | | Group C | | | | Group D | | |
|---|---|---|---|---|---|---|---|---|---|---|---|---|---|---|---|---|---|---|
| | | | KAERI | KEPRI | KTH | USNRC | CIAE | KNF | KOPEC1 | PSI | Univ. of Pisa | AEKI | EDO Gid. (GP1) | EDO Gid. (GP2) | EDO Gid. (GP3) | GRS | NRI | VTT |
| Primary system | | | | | | | | | | | | | | | | | | |
| Core power, MW | 1.635 | D1 | 1.635 | 1.566 | 1.636 | 1.553 | 1.613 | 1.636 | 1.633 | 1.638 | 1.636 | 1.636 | 1.636 | 1.635 | 1.636 | 1.636 | 1.636 | 1.64 |
| Pressure, MPa | 15.67 | D4 | 15.67 | 15.59 | 15.39 | 15.63 | 15.15 | 15.66 | 15.66 | 15.53 | 15.67 | 15.76 | 15.67 | 15.67 | 15.52 | 15.63 | 15.60 | 15.6 |
| Core inlet temp., K | 562.7 | D66 | 563.1 | 563.8 | 562.9 | 562.7 | 562.5 | 564.6 | 563.0 | 562.3 | 561.9 | 566.7 | 563.8 | 565.0 | 564.8 | 565.0 | 562.9 | 562.3 |
| Core exit temp., K | 597.7 | D67 | 598.2 | 598.5 | 598.3 | 598.5 | 597.3 | 598.2 | 596.4 | 597.4 | 596.6 | 597.7 | 599.0 | 598.8 | 597.8 | 598.4 | 597.2 | 595.5 |
| Bypass DC-UH, kg/s | ~0.0 | D95 | 0.0158 | -0.008 | 0.0 | 0.0 | 0.0 | -0.0185 | -0.0089 | -0.0336 | -0.1073 | 0.0027 | 0.1105 | 0.0 | 0.0 | -0.033 | 0.567 | -0.03 |
| Bypass DC-HL, kg/s | ~0.0 | D96 | 0.0178 | 0.0 | 0.0 | 0.0 | 0.0 | 0.0322 | 0.0011 | 0.0 | 0.0 | NA | 0.3478 | 0.0 | 0.0 | 7.5e-6 | 0.48 | 0.08 |
| CL flow rate, kg/s | 2.2 ± 5% | D99 | 1.9988 | 2.0068 | 1.9568 | 1.8469 | 2.017 | 2.0657 | 2.1098 | 2.0032 | 2.0306 | 2.2657 | 2.0412 | 2.0590 | 2.0433 | 2.11 | 2.18 | 2.1 |
| PZR level, m | 3.36 | D130 | 3.587 | 4.112 | 3.23 | 3.42 | 3.22 | 3.323 | 3.365 | 3.252 | 3.309 | 3.242 | 3.234 | 3.360 | 3.745 | 3.307 | 3.32 | 3.3 |
| RCP speed, rpm | 15 ± 5 | D139 | 22.2 | 223.9 | 21.5 | 200.5 | 24.0 | 263.9 | 30.0 | 23.3 | 11.6 | 0.0 | 0.0 | 0.0 | 0.0 | 10.7 | 18.9 | 19.2 |
| Secondary system | | | | | | | | | | | | | | | | | | |
| Pressure, MPa | 7.83 | D6 | 7.775 | 7.831 | 7.830 | 7.830 | 7.832 | 7.832 | 7.787 | 7.861 | 7.831 | 7.831 | 7.830 | 7.728 | 7.862 | 7.83 | 7.83 | 7.83 |
| Steam temp., K | 568.5 | D89 | 566.1 | 566.6 | 566.7 | 566.7 | 566.6 | 568.5 | 566.2 | 566.9 | 566.7 | 566.7 | 566.5 | 565.9 | 566.8 | 566.7 | 566.2 | 566.4 |
| Avg. FW temp., K | 508.2 | - | | 505.4 | 508.0 | 508.4 | | - | 505.4 | - | - | 508.0 | - | - | - | 508.2 | 507.2 | 508.2 |
| FW flow (ECO), kg/s | 0.43 | D103 | 0.455 | 0.3998 | 0.473 | 0.432 | 0.431 | 0.433 | 0.4639 | 0.4206 | 0.4326 | 0.4600 | 0.4382 | 0.4059 | 0.4566 | 0.432 | 0.431 | 0.42 |
| FW flow (DC), kg/s | ~0.0 | D104 | 0.0 | 0.0444 | 0.0 | 0.0 | 0.0 | 0.0 | 0.0 | 0.0 | 0.0 | 0.0 | 0.0 | 0.0 | 0.0 | 0.0 | 0.0 | 0 |
| SG level, m | 1.97~2.03 | - | | 4.08 | 3.44 | 1.83 | | - | 5.91 | - | - | 2.61 | - | - | - | 2.07 | 4.76 | 2.70 |
| Heat removal, kW | 753.67 | D2 | 815.8 | 781.17 | 815.46 | 777.06 | 784.17 | 810.82 | 816.97 | 750.92 | 772.94 | 813.18 | 791.96 | 796.80 | 817.54 | 786 | 730 | 775 |
| ECC | | | | | | | | | | | | | | | | | | |
| SIT pressure, MPa | 4.19 | D8 | 4.19 | 4.23 | 4.19 | 4.20 | 4.21 | 4.21 | 4.23 | 4.17 | 4.19 | 4.19 | 4.17 | 4.20 | 4.20 | 4.19 | 4.23 | 4.23 |
| SIP Temp., K | 321.3 | D82 | 323.3 | 320.9 | 325.1 | 323.3 | 323.3 | 323.3 | 323.2 | 320.2 | 323.0 | 323.2 | 322.9 | 323.1 | 323.2 | 323.2 | 323.2 | 321.3 |
| SIT Temp., K | 323.5 | D79 | 323.4 | 324.3 | 323.4 | 323.4 | 323.3 | 323.5 | 320.9 | 323.2 | 323.2 | 323.4 | 323.5 | 323.1 | 323.2 | 323.6 | 323.2 | 324.1 |
| SIT level, % | ~95 | - | | 95 | 95 | 95 | - | - | ~95 | - | - | ~95 | - | | | - | 95 | 95 |
| Containment | | | | | | | | | | | | | | | | | | |
| Pressure, MPa | 0.10 | D11 | 0.1013 | 0.1013 | 0.1029 | 0.1088 | 0.1013 | 0.1028 | 0.1029 | 0.1444 | 0.1013 | 0.1 | 0.1013 | 0.1000 | 0.0 | 0.1032 | 0.10 | 0.100 |